

# A Shape-Persistent Polyphenylene Spoked Wheel

Yi Liu,<sup>†</sup> Akimitsu Narita,<sup>†</sup> Joan Teyssandier,<sup>‡</sup> Manfred Wagner,<sup>†</sup> Steven De Feyter,<sup>‡</sup> Xinliang Feng,<sup>\*,§</sup> and Klaus Müllen<sup>\*,†</sup>

<sup>†</sup>Max Planck Institute for Polymer Research, Ackermannweg 10, 55128 Mainz, Germany

<sup>‡</sup>Division of Molecular Imaging and Photonics, Department of Chemistry, KU Leuven-University of Leuven, Celestijnenlaan 200 F, 3001 Leuven, Belgium

<sup>§</sup>Center for Advancing Electronics Dresden (cfaed) and Department of Chemistry and Food Chemistry, Technische Universität Dresden, Mommsenstrasse 4, 01062 Dresden, Germany

## Supporting Information

**ABSTRACT:** A shape-persistent polyphenylene with a “spoked wheel” structure was synthesized as a subunit of an unprecedented two-dimensional polyphenylene that we name graphenylene. The synthesis was carried out through a sixfold intramolecular Yamamoto coupling of a dodecabromo-substituted dendritic polyphenylene precursor, which had a central hexaphenylbenzene unit as a template. Characterizations by NMR spectroscopy and matrix-assisted laser ionization time-of-flight mass spectrometry provided an unambiguous structural proof for the wheel-like molecule with a molar mass of 3815.4 g/mol. Remarkably, scanning tunneling microscopy visualization clearly revealed the defined spoked wheel structure of the molecule with six internal pores.

Two-dimensional (2D) carbon-based materials have attracted enormous interest in recent decades because of their unique structures, intriguing properties, and versatile applications,<sup>1–4</sup> especially after the landmark advent of graphene.<sup>5</sup> With the combination of  $sp$ -,  $sp^2$ -, and  $sp^3$ -hybridized carbon atoms, a number of 2D carbon materials with different architectures have also been synthesized and/or theoretically predicted.<sup>2,6–18</sup> In particular, graphene has attracted major attention during the past decade, which also stimulated studies of other 2D carbon materials such as  $\gamma$ -graphyne and graphdiyne (Figure 1).<sup>10,11,14,19,20</sup> Atomically precise syntheses of  $\gamma$ -graphyne and graphdiyne remain elusive, but widely studied phenylene ethynylene-based macrocycles can be regarded as their molecular subunits.<sup>21–25</sup>

The electronic properties of 2D carbon materials are critically dependent on the composition and arrangement of the  $sp$ -,  $sp^2$ -, and/or  $sp^3$ -hybridized carbon atoms. For example, while graphene is a zero-band-gap semimetal,  $\gamma$ -graphyne and graphdiyne are both predicted to be semiconductors with open band gaps.<sup>12</sup> Moreover, theoretical studies elucidate that graphdiyne has an excellent intrinsic electron mobility reaching  $10^5 \text{ cm}^2 \text{ V}^{-1} \text{ s}^{-1}$ .<sup>12</sup> Further exploration of the structural diversity of 2D carbon architectures is expected to furnish materials with unique and tunable properties. Nevertheless, the number of reported examples of 2D carbon materials is still limited.<sup>2,6–18</sup>

By replacement of the ethynylene groups of  $\gamma$ -graphyne and graphdiyne with  $p$ -phenylene units, two purely  $sp^2$ -hybridized

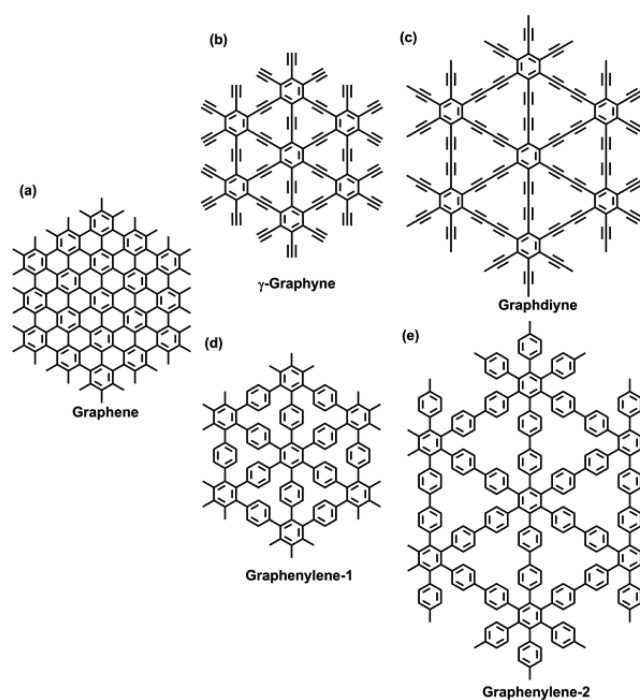


**Figure 1.** Structural representations of 2D carbon materials: (a) graphene, (b)  $\gamma$ -graphyne, (c) graphdiyne, and two newly proposed, purely  $sp^2$ -hybridized structures, (d) graphenylene-1 and (e) graphenylene-2.

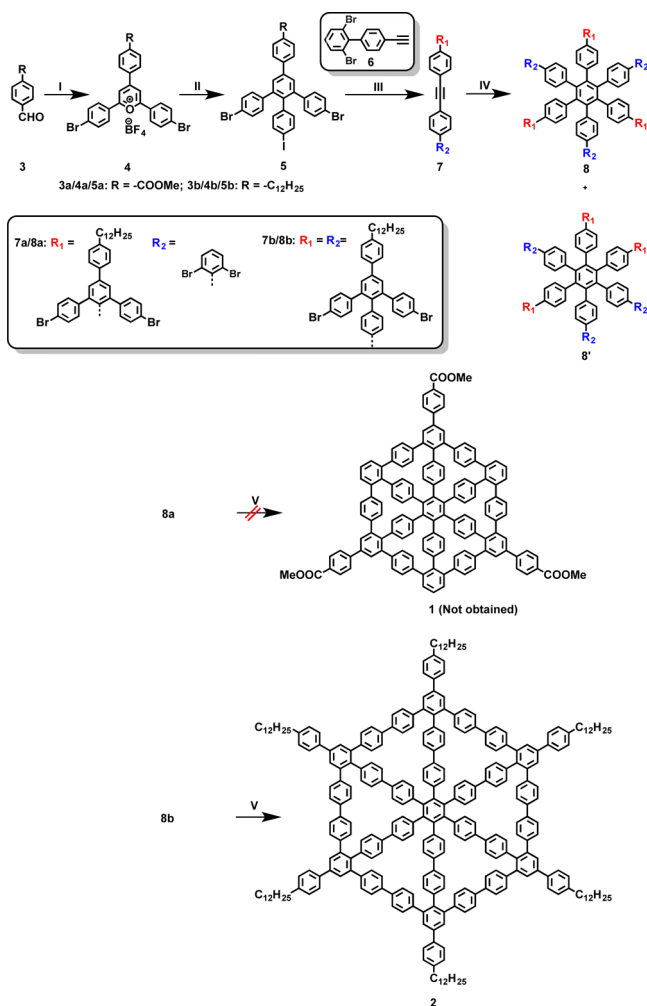
2D carbon structures with hexagonal symmetry can be conceived, which we name graphenylene-1 and graphenylene-2, respectively (Figure 1). Notably, graphenylene-1 corresponds to a single-layer substructure of the hypothetical carbon allotrope “cubic graphite”,<sup>26</sup> the synthesis of which still remains elusive. Because the direct and precise fabrication of these 2D carbon architectures is also highly challenging, we start with the synthesis of their subunits with defined sizes and shapes. During the past decade, Höger and co-workers have developed elegant modular syntheses of large and shape-persistent “molecular spoked wheels” consisting of phenylene ethynylene units and having diameters reaching  $\sim 12 \text{ nm}$ .<sup>27,28</sup> Adapting

Received: October 4, 2016

Published: November 16, 2016

their modular protocol, we designed synthetic routes toward two polyphenylene spoked wheels, **1** and **2**, consisting of 22 and 37 benzene rings, as nanosized subunits of graphenylene-1 and graphenylene-2, respectively (Scheme 1). Although the

Scheme 1. Synthetic Route toward Compounds **1** and **2**<sup>a</sup>



<sup>a</sup>Reagents and conditions: (i) 4-bromoacetophenone, BF<sub>3</sub>·Et<sub>2</sub>O, 100 °C, 12 h; **4a**, 25%; **4b**, 46%; (ii) sodium 4-iodophenacetate, Ac<sub>2</sub>O, 150 °C, 12 h; **5a**, 47%; **5b**, 39%; (iii) **7a**: **6**, Pd(PPh<sub>3</sub>)<sub>2</sub>Cl<sub>2</sub>, Et<sub>3</sub>N, THF, 12 h, rt, 71%; **7b**: 1,2-bis(4-(4,4,5,5-tetramethyl-1,3,2-dioxaborolan-2-yl)phenyl)acetylene, Pd(PPh<sub>3</sub>)<sub>4</sub>, K<sub>2</sub>CO<sub>3</sub>, THF, methanol/H<sub>2</sub>O, 12 h, 60 °C, 58%; (iv) Co<sub>2</sub>(CO)<sub>8</sub>, toluene, refluxing; **8a**, 23%; **8b**, 34%; (v) Ni(COD)<sub>2</sub>, COD, bipyridine, THF, 120 °C, microwave reactor; **1**, 0%; **2**, 58%. Abbreviations: THF, tetrahydrofuran; COD, 1,5-cyclo-octadiene.

preparation of **1** turned out to be elusive by the current method because of the high steric hindrance in the final ring-forming step, **2** was obtained and unambiguously characterized by NMR spectroscopy, mass spectrometry, and scanning tunneling microscopy (STM). Compound **2** has a D<sub>6h</sub>-symmetric structure and is expected to be highly shape-persistent with its rigid polyphenylene backbone.

Toward the synthesis of **1** and **2**, dendritic polyphenylene precursors **8a** and **8b**, respectively, were designed with 12 bromo groups at appropriate positions for forming the rims of the wheel-like molecules by sixfold aryl–aryl coupling reactions. The hexaphenylbenzene core is expected to serve as a shape-

persistent template that facilitates the ring closure. Precursors **8a** and **8b** can be synthesized through cobalt-catalyzed cyclotrimerization of the corresponding alkynes **7a** and **7b**. On the one hand, **8a** with C<sub>3</sub> symmetry will be inevitably mixed with its undesired constitutional isomer **8a'** (Scheme 1). We therefore introduced strongly polar benzoate groups at the peripheral phenyl rings of precursor **8a** to enable its isolation by column chromatography. On the other hand, **8b** with C<sub>6</sub> symmetry can be obtained as a single isomer and does not require polar groups for the isolation.

Dendritic polyphenylene precursor **8a** was prepared over four steps as shown in Scheme 1 and could be easily separated from its undesired regioisomer **8a'** by silica gel column chromatography. Matrix-assisted laser ionization time-of-flight (MALDI-TOF) mass spectrometry (MS), <sup>1</sup>H NMR spectroscopy, <sup>1</sup>H–<sup>1</sup>H 2D correlation spectroscopy (COSY), and nuclear Overhauser enhancement spectroscopy (NOESY) validated the chemical identity of **8a** (see the Supporting Information). Yamamoto coupling of precursor **8a** was then attempted under various conditions, including the use of a microwave reactor (see Table S1), but failed to give the desired compound **1**, most probably because of steric hindrance of the *o*-bromobiphenyl unit of **8a**.

In order to circumvent the steric problem in the last cyclization step, compound **2** was next targeted, replacing the phenylene bridges of **1** with biphenylene units. The synthesis of **2** was performed as shown in Scheme 1 following a similar strategy as the one toward **1**. Suzuki coupling of freshly prepared 9-dodecyl-9-borabicyclo(3.3.1)nonane with 4-bromobenzaldehyde gave 4-dodecylbenzaldehyde (**3b**), which was then subjected to Lewis acid-catalyzed condensation with 4-bromoacetophenone to yield triphenylpyrium salt **4b**. Condensation of **4b** with sodium 4-iodophenacetate in refluxing acetic anhydride provided oligophenylene **5b**, and then Suzuki coupling between **5b** and 1,2-bis(4-(4,4,5,5-tetramethyl-1,3,2-dioxaborolan-2-yl)phenyl)acetylene furnished alkyne **7b**. The dendritic precursor **8b** was obtained by cobalt-catalyzed cyclotrimerization of **7b** in refluxing toluene (Scheme 1). MALDI-TOF MS and <sup>1</sup>H NMR analyses proved the chemical identity of precursor **8b** (Figures S28 and S29).

In contrast to the unsuccessful synthesis of **1**, the intramolecular ring closure of precursor **8b** to form compound **2** was efficiently achieved by nickel-catalyzed coupling under microwave treatment. This was most probably due to the reduced steric hindrance and the absence of the *o*-bromobiphenyl moiety in precursor **8b**, in comparison with the more congested precursor **8a**. Preparative gel-permeation chromatography (GPC) enabled complete purification, providing **2** in 56% yield as a colorless solid. The MALDI-TOF MS spectrum of **2** indicated the presence of a single species with *m/z* = 3815.5, consistent with the desired molar mass of 3815.4 g/mol, and the experimental isotopic distribution was in perfect agreement with the simulated pattern (Figure 2).

<sup>1</sup>H NMR together with 2D COSY and NOESY spectra provided further structural proof for compound **2**, where every aromatic proton signal could be unambiguously assigned (Figures 3, S9, and S10). The <sup>1</sup>H NMR spectrum showed that only the signals from H<sub>e</sub>, H<sub>g</sub>, and H<sub>h</sub> were slightly upfield-shifted from 7.48, 7.23, and 7.20 ppm to 7.42, 7.15, and 7.14 ppm, respectively, when the temperature was raised from 298 to 366 K. This is presumably because these protons point out of the plane at room temperature because of steric repulsion but have higher freedom of rotation at an elevated temperature,

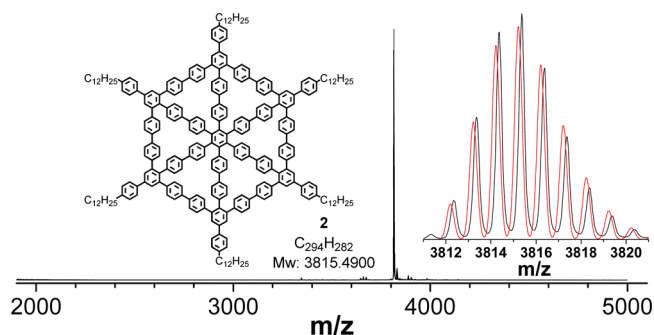


**Figure 2.** MALDI-TOF MS spectrum of **2**. Inset: isotopic distribution (black) compared with the simulated mass spectrum (red) for  $C_{294}H_{282}$ .

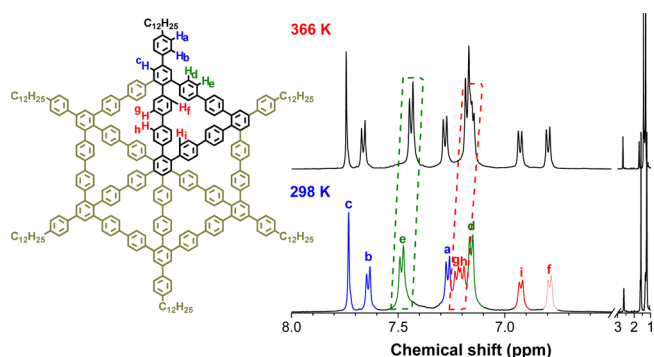


**Figure 3.**  $^1H$  NMR spectrum of **2** in  $C_2D_2Cl_4$  at room temperature with the assignment of aromatic protons.

leading to a reduced deshielding effect from the adjacent phenylene ring. Furthermore, on the basis of the NMR diffusion-ordered spectroscopy (DOSY) measurement on **2** (Figure S11) with a calculated self-diffusion constant ( $D$ ) of  $7.06 \times 10^{-11} \text{ m}^2 \text{ s}^{-1}$ , the diameter of **2** in tetrachloroethane was estimated to be 3.89 nm, which is comparable to the theoretical molecular size of the polyphenylene core of **2** (3.74 nm) calculated by density functional theory (DFT) at the B3LYP/6-31G(d) level (Figure S4).

The theoretically calculated geometry of **2** (DFT, B3LYP/6-31G(d)) clearly showed that its polyphenylene backbone is confined into a two-dimensional plane, in contrast to three-dimensional polyphenylene dendrimers. Six “rimlike” biphenylene units are supported by six “spokelike” biphenylene segments, and they are all tilted out of the plane (Figures S3 and S4). The UV–vis absorption spectrum of **2** displays a slight blue shift of  $\sim 10$  nm relative to that of precursor **7b**, which is presumably due to a decrease in the effective conjugation length of the  $p$ -oligophenylene units as a result of the tilting (Figure S2a). Indeed, the absorption spectrum of **2** is similar to those of cyclic nonaphenylene derivatives reported by Iyoda and co-workers,<sup>29</sup> suggesting interruption of the  $\pi$  conjugation. On the other hand, the fluorescence spectra display a red shift and a larger Stokes shift for **2** ( $\lambda_{fl} = 422$  nm, with a shift of 125 nm) compared with those of **8b** ( $\lambda_{fl} = 393$  nm, with a shift of 83 nm) (Figure S2c), which suggests that the excited state of **2** has a more planarized structure than that of **8b**, with extended  $\pi$  conjugation in contrast to their ground-state structures.

To confirm the shape-persistent nature of the wheel-like molecule, a self-assembled monolayer of **2** was characterized at submolecular resolution using STM at the 1-phenyloctane/highly oriented pyrolytic graphite (HOPG) interface at room

temperature (Figure 4). Wheel-like molecule **2** formed a hexagonal 2D pattern on the substrate with unit cell parameters

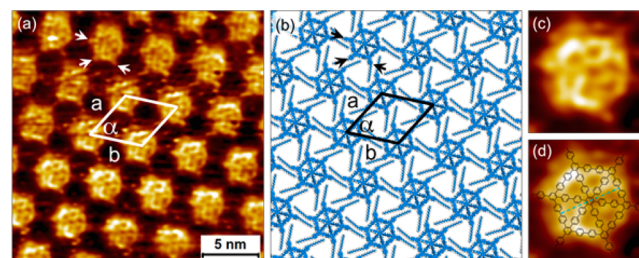


**Figure 4.** (a) High-resolution STM image of a self-assembled monolayer of **2**. The unit cell parameters are  $a = b = 4.7 \pm 0.2$  nm and  $\alpha = 60 \pm 3.0^\circ$  (one molecule per unit cell). Tunneling current,  $I_{set} = 25$  pA; sample bias,  $V_{bias} = -1.5$  V. (b) Molecular model of the self-assembled network of **2**. (c) Digital zoom (4.1 nm  $\times$  4.1 nm) of the STM image in (a) showing the aromatic core of a single molecule of **2**. (d) Same image as in (c) but overlapped with the molecular structure of **2**.

of  $a = b = 4.7 \pm 0.2$  nm and  $\alpha = 60 \pm 3^\circ$ . Figure 4a shows a high-resolution STM image of the monolayer, in which submolecular features within the aromatic part of the molecular spoked wheel are clearly visible. The conjugated polyphenylene cores appear as bright spoked wheels separated by darker regions wherein the peripheral dodecyl chains are adsorbed.

A molecular model built using the experimentally obtained lattice parameters (Figure 4b) reveals that the dodecyl chains possibly interact with each other via van der Waals interactions. The model also shows that the regions between the dodecyl chains are largely empty, and thus, they are possibly filled by mobile solvent molecules. The dimension of the polyphenylene core obtained from calibrated STM images ( $\sim 2.4$  nm, as indicated by the dashed line in Figure 4d) matches closely with the one obtained from the theoretically calculated structure (2.2 nm). Furthermore, the STM contrast of the aromatic core matches closely with the anticipated structure of **2**. Each bright feature consists of a hexagonal frame (“rimlike” biphenylenes) filled with a star-shaped feature (“spokelike” biphenylenes) with a central dark blob. The “spokelike” biphenylenes give rise to six adjacent pores, as expected from the molecular structure (Figure 4c,d). The tilted biphenylenes presumably enhance the self-assembly by multiple  $CH-\pi$  interactions with the graphite surface. The peripheral phenyl rings that form a part of the phenyldodecyl substitution are also visualized (arrows in Figure 4a,b). Thus, the STM analysis not only proved the chemical structure of the targeted compound **2** but also provided direct evidence for its shape-persistent conformation on a solid substrate, which was not accessible via conventional characterization methods.

In summary, we considered two 2D carbon architectures, graphenylene-1 and graphenylene-2, with hexagonal symmetry by replacing ethynyl groups of  $\gamma$ -graphyne and graphdiyne, respectively, with  $p$ -phenylene linkages and synthesized the shape-persistent polyphenylene spoked wheel **2** corresponding to a subunit of graphenylene-2. With the assistance of the hexaphenylbenzene core as the cyclization template, the macrocyclic backbone of **2** was constructed via sixfold intramolecular nickel-catalyzed coupling in high yield. Remarkably, a submolecular-resolution STM image was obtained at the liquid–solid interface that clearly elucidated the shape-persistent “spoked wheel” structure of **2**. Such a molecular



structure with six internal pores (approximately 4 Å in diameter as measured both in models and STM images) can be highly interesting for studying supramolecular interactions with other guest molecules or ions, since they are expected to accommodate, e.g., methyl groups or Br<sup>-</sup> or I<sup>-</sup> anions. These results open up a new avenue for designing and synthesizing a further variety of unprecedented 2D carbon structures and their subunits.

## ■ ASSOCIATED CONTENT

### Supporting Information

The Supporting Information is available free of charge on the ACS Publications website at DOI: 10.1021/jacs.6b10369.

Experimental details; cyclic voltammograms; NMR, UV–vis absorption, fluorescence, and MALDI-TOF MS spectra; and additional STM images and molecular models (PDF)

## ■ AUTHOR INFORMATION

### Corresponding Authors

\*xinliang.feng@tu-dresden.de

\*muellen@mpip-mainz.mpg.de

### ORCID

Klaus Müllen: 0000-0001-6630-8786

### Notes

The authors declare no competing financial interest.

## ■ ACKNOWLEDGMENTS

We are grateful for the financial support from the European Research Council grant on NANOGRAPH as well as under the European Union's Seventh Framework Programme (FP7/2007-2013)/ERC Grant Agreement 340324, the European Commission through the FET Project UPGRADE (GA-309056) and Graphene Flagship (CNECT-ICT-604391), and DFG Priority Program SPP 1459.

## ■ REFERENCES

- (1) Geim, A. K.; Novoselov, K. S. *Nat. Mater.* **2007**, *6*, 183.
- (2) Segawa, Y.; Ito, H.; Itami, K. *Nat. Rev. Mater.* **2016**, *1*, 15002.
- (3) Pinzón, J. R.; Villalta-Cerdas, A.; Echegoyen, L. In *Unimolecular and Supramolecular Electronics I: Chemistry and Physics Meet at Metal–Molecule Interfaces*; Metzger, M. R., Ed.; Springer: Berlin, 2012; p 127.
- (4) Jariwala, D.; Sangwan, V. K.; Lauhon, L. J.; Marks, T. J.; Hersam, M. C. *Chem. Soc. Rev.* **2013**, *42*, 2824.
- (5) Novoselov, K. S.; Geim, A. K.; Morozov, S. V.; Jiang, D.; Zhang, Y.; Dubonos, S. V.; Grigorieva, I. V.; Firsov, A. A. *Science* **2004**, *306*, 666.
- (6) Falcao, E. H. L.; Wudl, F. *J. Chem. Technol. Biotechnol.* **2007**, *82*, 524.
- (7) Georgakilas, V.; Perman, J. A.; Tucek, J.; Zboril, R. *Chem. Rev.* **2015**, *115*, 4744.
- (8) Zhang, S.; Zhou, J.; Wang, Q.; Chen, X.; Kawazoe, Y.; Jena, P. *Proc. Natl. Acad. Sci. U. S. A.* **2015**, *112*, 2372.
- (9) Sharma, B. R.; Manjanath, A.; Singh, A. K. *Sci. Rep.* **2014**, *4*, 7164.
- (10) Li, Y.; Xu, L.; Liu, H.; Li, Y. *Chem. Soc. Rev.* **2014**, *43*, 2572.
- (11) Hirsch, A. *Nat. Mater.* **2010**, *9*, 868.
- (12) Diederich, F.; Rubin, Y. *Angew. Chem., Int. Ed. Engl.* **1992**, *31*, 1101.
- (13) Diederich, F. *Nature* **1994**, *369*, 199.
- (14) Baughman, R. H.; Eckhardt, H.; Kertesz, M. *J. Chem. Phys.* **1987**, *87*, 6687.
- (15) Bieri, M.; Treier, M.; Cai, J.; Ait-Mansour, K.; Ruffieux, P.; Groning, O.; Groning, P.; Kastler, M.; Rieger, R.; Feng, X.; Müllen, K.; Fasel, R. *Chem. Commun.* **2009**, 6919.
- (16) Eichhorn, J.; Nieckarz, D.; Ochs, O.; Samanta, D.; Schmittel, M.; Szabelski, P. J.; Lackinger, M. *ACS Nano* **2014**, *8*, 7880.
- (17) Klappenberger, F.; Zhang, Y.-Q.; Björk, J.; Klyatskaya, S.; Ruben, M.; Barth, J. V. *Acc. Chem. Res.* **2015**, *48*, 2140.
- (18) Li, Q.; Yang, B.; Lin, H.; Aghdassi, N.; Miao, K.; Zhang, J.; Zhang, H.; Li, Y.; Duhm, S.; Fan, J.; Chi, L. *J. Am. Chem. Soc.* **2016**, *138*, 2809.
- (19) Malko, D.; Neiss, C.; Viñes, F.; Görling, A. *Phys. Rev. Lett.* **2012**, *108*, 086804.
- (20) Zhou, J.; Gao, X.; Liu, R.; Xie, Z.; Yang, J.; Zhang, S.; Zhang, G.; Liu, H.; Li, Y.; Zhang, J.; Liu, Z. *J. Am. Chem. Soc.* **2015**, *137*, 7596.
- (21) Bhaskar, A.; Guda, R.; Haley, M. M.; Goodson. *J. Am. Chem. Soc.* **2006**, *128*, 13972.
- (22) Haley, M. M.; Brand, S. C.; Pak, J. J. *Angew. Chem., Int. Ed. Engl.* **1997**, *36*, 836.
- (23) Iyoda, M.; Yamakawa, J.; Rahman, M. J. *Angew. Chem., Int. Ed.* **2011**, *50*, 10522.
- (24) Bunz, U. H. F.; Rubin, Y.; Tobe, Y. *Chem. Soc. Rev.* **1999**, *28*, 107.
- (25) Tahara, K.; Yoshimura, T.; Sonoda, M.; Tobe, Y.; Williams, R. V. *J. Org. Chem.* **2007**, *72*, 1437.
- (26) Baughman, R. H.; Cui, C. *Synth. Met.* **1993**, *55*, 315.
- (27) May, R.; Jester, S.-S.; Höger, S. *J. Am. Chem. Soc.* **2014**, *136*, 16732.
- (28) Mössinger, D.; Hornung, J.; Lei, S.; De Feyter, S.; Höger, S. *Angew. Chem., Int. Ed.* **2007**, *46*, 6802.
- (29) Rahman, M. J.; Yamakawa, J.; Matsumoto, A.; Enozawa, H.; Nishinaga, T.; Kamada, K.; Iyoda, M. *J. Org. Chem.* **2008**, *73*, 5542.